Origin of Carbon Monoxide Formation in the Oxidative Dehydrogenation of Propane Using Carbon Dioxide

James H. Carter,* Tongqi Ye, Daniel G. Hewes, Ahlam Almoteiry, Kieran J. Aggett, Bart D. Vandegehuchte, Christopher J. Kiely, Stuart H. Taylor, and Graham J. Hutchings*

Read Online

ACCESS | Metrics & More | Article Recommendations | Supporting Information

ABSTRACT: The oxidative dehydrogenation of C_3H_8 to C_3H_6 using CO_2 is an attractive alternative to nonoxidative propane dehydrogenation and facilitates the utilization of CO_2. The activity of supported nanoparticles for this reaction has been extensively investigated, but the often-overlooked deleterious formation of CO via reforming reactions remains a challenge with these catalysts. In this paper, we investigate the origin of CO formation over supported nanoparticle catalysts and find that the support and metal both play a role in favoring the formation of either CO or C_3H_6. Reducible supports are associated with higher activity and increased CO formation, but nonreducible supports also facilitate CO formation. Supported Pt catalysts were more selective toward C_3H_6 than Pd analogues, but both catalysts favored coke formation. These findings highlight the need for careful catalyst design in supported nanoparticle catalysts for the oxidative dehydrogenation of propane using carbon dioxide, particularly with respect to tuning catalyst selectivity.

KEYWORDS: oxidative dehydrogenation, propane, dehydrogenation, propene, carbon dioxide, reforming
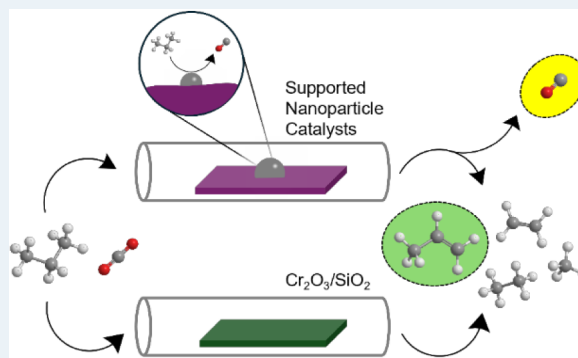
INTRODUCTION

The direct dehydrogenation of propane (DDH) is an established commercial process that offers a more efficient pathway to propene than steam cracking and fluid catalytic cracking, which form propene as a byproduct.[1−4] Propene is a major platform chemical used as a precursor to polypropene, acetonitrile, propene oxide, and acrylic acid, among others. Annual production of propene was around 130 million tonnes in 2019.[5] The interest in DDH increased significantly with the acknowledgment that existing production capacity could not keep pace with increasing demand, hence the emergence of the "propene gap". DDH is helping to fill that gap and has been commercialized by several companies that utilize various catalysts, including Pt−Sn, Pt−Ga, and CrO_x.[6−10] These on-purpose processes still produce a minority of propene compared to the refinery processes mentioned above, but their importance in the propene production landscape is expected to grow significantly in the coming decades. Furthermore, DDH processes enable the use of renewable propane (biopropane), not just petrochemical feedstocks.[11] As society shifts from relying on fossil fuels to developing renewable energy sources, such sustainable feedstocks will be very important.

Commercial DDH processes suffer from coking on-stream and require complex and frequent regeneration cycles to maintain propene production.[10,12−14] Consequently, the addition of an oxidant such as O_2 (ODH−O_2) and CO_2 (ODH−CO_2) has been explored in recent years. Notable advances in ODH−O_2 have been made, namely by Hermans and coworkers, who reported the exceptional activity of boron catalysts.[15−19] In terms of propene production, these catalysts compete with the most active Pt and CrO_x catalysts in the literature for DDH.[12]

ODH−CO_2 offers the advantage of utilizing CO_2 in the process, which has obvious benefits from an environmental and sustainability point of view, as long as the primary product of CO_2 utilization (CO) can be accounted for downstream and not simply combusted. There have been many investigations into ODH−CO_2 since it was first reported by Takahara et al. in 1996, who showed that supported chromium oxide (CrO_x) catalysts were highly selective toward propene at 600 °C.[20] A strong support effect was observed, whereby the addition of CO_2 was beneficial for CrO_x/SiO_2, but for CrO_x/Al_2O_3 the catalyst was inhibited. An inhibition effect of CO_2 was also observed over CrO_x/Al-beta[21] and Ga_2O_3/Al_2O_3[22] (for the
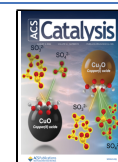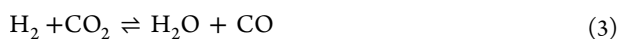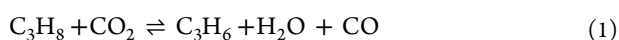
Table 1. Summary of the Literature on ODH−CO$_2$ and Their References to Reforming Reactions, the Inclusion of CO as a Potential Reaction Product from Propane Conversion, and the Method Used to Calculate Selectivity

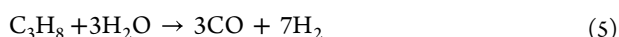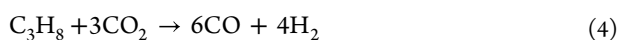| catalyst(s)	category	is reforming mentioned?	CO as a product?	selectivity method[a]	year	ref
Mo$_2$C	carbide	Y	Y	3	2018	[33]
Ni−CrO$_x$/SiO$_2$	chromium	Y	?	0	2012	[34]
CrO$_x$/ZrO$_2$	chromium	N	?	3	2015	[35]
CrO$_x$/ C	chromium	N	N	1	2008	[36]
CrO$_x$/SiO$_2$	chromium	N	N	3	2019	[37]
CrO$_x$/SiO$_2$	chromium	N	N	3	2016	[38]
CrO$_x$/ZrO$_2$	chromium	N	Y	3	2018	[39]
CrO$_x$/ZSM-5	chromium	N	N	0	2011	[40]
silica-supported CrO$_x$	chromium	N	N	1	2011	[41]
Cr/beta-zeolite	chromium	N	N	3	2020	[21]
CrO$_x$−Al$_2$O$_3$	chromium	Y	N	1	1996	[20]
CrO$_x$−ZrO$_2$	chromium	N	N	3	2013	[42]
CrO$_x$/SiO$_2$	chromium	N	N	1	2012	[43]
CrO$_x$/MCM-41	chromium	N	N	1	2008	[23]
CrO$_x$/SBA-15	chromium	N	N	1	2010	[44]
supported CrO$_x$	chromium	N	Y	0	2002	[45]
CrO$_x$/silicalite-1,B-MFI	chromium	N	N	1	2011	[46]
CrO$_x$/SiO$_2$	chromium	N	N	0	2016	[47]
CrO$_x$/SiO$_2$	chromium	N	N	0	2006	[48]
CrO$_x$−ZrO$_2$	chromium	N	Y	3	2019	[49]
CrO$_x$/SBA-1	chromium	N	N	1	2012	[24]
metal oxide/MCM-41	chromium	N	N	0	2004	[50]
RuCrO$_x$/SiO$_2$	chromium	Y	Y	3	2020	[51]
CrO$_x$/CeZrO$_x$	chromium	Y	N	1	2023	[52]
GaO$_x$	gallium	N	N	3	2006	[53]
CrO$_x$/β-gallia	gallium	N	N	0	2006	[54]
Ga$_2$O$_3$/HZSM-48,ZSM-5	gallium	N	N	0	2012	[55]
Ga$_2$O$_3$/TiO$_2$, ZrO$_2$, MgO	gallium	N	N	3	2006	[53]
Ga$_2$O$_3$−Al$_2$O$_3$	gallium	N	N	3	2013	[56]
Ga$_2$O$_3$−Al$_2$O$_3$	gallium	N	N	0	2008	[26]
Ga$_2$O$_3$−Al$_2$O$_3$	gallium	N	N	0	2008	[25]
GaN/SiO$_2$	gallium	N	N	3	2020	[57]
gallium oxides	gallium	N	N	3	2005	[58]
Ga$_2$O$_3$−Al$_2$O$_3$	gallium	N	N	1	2023	[59]
α-NiMoO$_4$	metal oxide	N	N	0	2003	[60]
supported Fe$_2$O$_3$	metal oxide	Y	N	0	2004	[30]
In/ZSM-5	metal oxide	N	Y	2	2020	[27]
In$_2$O$_3$/Mo$_x$ (M = Al, Zr, Si)	metal oxide	N	N	0	2011	[28]
In$_2$O$_3$−Al$_2$O$_3$	metal oxide	N	N	3	2010	[61]
doped-In$_2$O$_3$	metal oxide	N	N	0	2010	[62]
Mo$_2$C/SiO$_2$	metal oxide	N	N	0	2001	[63]
NiMoO$_4$	metal oxide	N	N	0	2002	[64]
V-MCM-41	metal oxide	N	N	3	2018	[29]
VO$_x$/SiO$_2$	metal oxide	N	Y?	0	2017	[65]
WO$_x$−VO$_x$/SiO$_2$	metal oxide	N	N	0	2016	[66]
ZnO/ZSM-5	metal oxide	N	N	0	2009	[31]
Mo−ZnO/ZrO$_2$	metal oxide	Y	Y	3	2024	[67]
Zn−Fe/S-1	metal oxide	Y	N	1	2023	[68]
VO$_x$/In$_2$O$_3$	metal oxide	N	N	0	2023	[69]
PtSn/SiO$_2$	nanoparticle	Y	Y	1	2023	[70]
Au/MgO, ZnO, Al$_2$O$_3$	nanoparticle	Y	Y	3	2016	[71]
FeNi and FePt/CeO$_2$	nanoparticle	Y	Y	3	2018	[72]
Pd/CZA	nanoparticle	N	N	1	2018	[32]
Re/ZSM-5	nanoparticle	N	N	3	2005	[73]
Ru/ZrO$_2$, CeO$_2$	nanoparticle	Y	Y	3	2016	[74]
Ni−X/CeO$_2$	nanoparticle	Y	Y	3	2019	[75]
Pt−Sn/CeO$_2$	nanoparticle	Y	Y	3	2023	[76]

[a]Selectivity calculations based on 0 = not enough information given, 1 = observed products (no CO), 2 = observed products (with CO), and 3 = converted propane.

ODH−CO$_2$ of ethane), which suggests that the Al component of the support was responsible for the poor performance. The presence of basic sites on Al$_2$O$_3$ may be responsible for the strong adsorption of CO$_2$, and the majority of supported CrO$_x$ investigations use various forms of SiO$_2$ as a result.[21−24] Ga$_2$O$_3$,[25,26] In$_2$O$_3$,[27,28] VO$_x$,[29] Fe$_2$O$_3$,[30] and ZnO[31] have also been examined for ODH−CO$_2$, but the most promising catalysts are typically an order of magnitude below those of DDH or ODH−O$_2$ catalysts in terms of space-time yield.[12]

The addition of CO$_2$ to the reaction mixture has been proposed to function in two ways. First, CO$_2$ can provide surface O species that directly abstract H from propane via a Mars−van Krevelen mechanism, similar to conventional oxidative dehydrogenation catalysts. Second, CO$_2$ can facilitate the reverse water−gas shift reaction (RWGS), which removes H$_2$ from the reaction, freeing up active sites and crucially shifting the thermodynamic equilibrium favorably toward producing propene. These pathways are known as direct (eq 1) and indirect (eqs 2 and 3), respectively.

$$C_3H_8 + CO_2 \rightleftharpoons C_3H_6 + H_2O + CO \tag{1}$$

$$C_3H_8 \rightleftharpoons C_3H_6 + H_2 \tag{2}$$

$$H_2 + CO_2 \rightleftharpoons H_2O + CO \tag{3}$$

The extent to which each pathway operates depends on the catalyst, and these pathways do not need to be mutually exclusive.[32] In addition to the pathways mentioned above, there are various side-reactions that can take place under typical reaction conditions. These include dry reforming (eq 4), steam reforming (eq 5), cracking (eq 6), and deep dehydrogenation to coke. In the case of deep dehydrogenation to coke, it has been reported that CO$_2$ inhibits this via the reverse Boudouard reaction (eq 7).[12] Finally, the methanation of CO$_2$ and CO can take place using H$_2$ generated in the reaction (eqs 8 and 9).

$$C_3H_8 + 3CO_2 \rightarrow 6CO + 4H_2 \tag{4}$$

$$C_3H_8 + 3H_2O \rightarrow 3CO + 7H_2 \tag{5}$$

$$C_3H_8 \rightarrow CH_4 + C_2H_4 \tag{6}$$

$$C + CO_2 \rightleftharpoons 2CO \tag{7}$$

$$CO_2 + 4H_2 \rightarrow CH_4 + 2H_2O \tag{8}$$

$$CO + 3H_2 \rightarrow CH_4 + H_2O \tag{9}$$

While the rate of these side-reactions in ODH−CO$_2$ is dependent on the catalyst, they are too frequently overlooked in the literature, with CO-forming reactions (i.e., dry reforming, steam reforming, reverse Boudouard) in particular not being accounted for in selectivity calculations. Careful examination of the literature on the topic of ODH−CO$_2$ (56 available peer-reviewed articles) revealed that 75% do not mention reforming at all in the article. Regarding the calculation of selectivity in the reaction, 41% of articles calculate it based on converted propane, which is preferable, but of these articles, less than half (43%) consider CO as a potential product. 22% of articles calculate selectivity based on observed products, which, with one exception, do not include CO as a product. Finally, 35% of articles do not disclose the calculation for selectivity at all. Overall, this demonstrates that the importance of CO-forming reactions in ODH−CO$_2$ has been somewhat neglected, which may lead to the presentation of misleading propene selectivity values. Table 1[34−36] summarizes the literature reports showing where reforming was mentioned, CO was considered as a potential product, and what was the methodology for calculating selectivity to C$_3$H$_6$. The purpose of including this table is not to highlight research reports where potentially misleading reaction selectivities have been reported but to highlight the different approaches being taken by different research groups in determining reaction selectivities on the range of catalysts studied to date and thereby demonstrate where the different methodologies could result in misleading conclusions. Of the methodologies reported, the most robust one is method 3 (considering the converted C$_3$H$_8$ as the basis for C$_3$H$_6$ selectivity). Method 2 (observed products including CO) is less preferable as it leaves the possibility of certain products not being detected and possibly leads to inflated selectivity values. Method 1, where observed products not including CO are used, is the most prone to give misleading results as CO could constitute the major product but is not accounted for. That said, if CO was not formed during the reaction, then the selectivity calculation would be accurate.

In the first report of supported Pd catalysts for ODH−CO$_2$ of C$_3$H$_8$, Nowicka et al. reported that Pd/CeZrAlO$_x$ catalysts can efficiently dissociate CO$_2$ on the surface and produce C$_3$H$_6$ at 450 °C, with selectivity approaching 90%.[32] However, the selectivity was calculated based on observed products (i.e., method 1) and without considering that CO could be formed from C$_3$H$_8$. Therefore, the extent of dry (or steam) reforming was not measured. On the other hand, Gomez et al. observed dry reforming to be prevalent over CeO$_2$-supported metal nanoparticle (NP) catalysts.[72,75] It was shown that certain bimetallic catalyst formulations, namely Ni$_3$−Pt$_1$, Fe$_1$−Ni$_3$, and Co$_3$−Pt$_1$ mostly catalyzed CO formation while Fe$_3$−Pd$_1$ and Fe$_3$−Ni$_1$ favored dehydrogenation and/or cracking pathways, although in all cases both reactions were observed. This underlines the importance of considering CO-forming reactions and calculating selectivity on the basis of converted propane. As recognized by Wang et al. in their investigation into Fe−CeO$_2$ catalysts for ODH−CO$_2$, it is not trivial to untangle these reactions.[77] CO can be formed from five different reactions (eqs 1, 3−5, and 7) and has also been reported to form via (incomplete) combustion of C$_3$H$_8$ at higher temperatures, i.e., 600 °C.

Xing et al. recently reported that PtCoIn/CeO$_2$ and a high-entropy intermetallic catalyst (PtCoNiSnInGa supported on CeO$_2$) were efficient ODH−CO$_2$ catalysts.[78,79] The catalysts exhibited C$_3$H$_6$ yields that were as high as or outperformed those of the state-of-the-art catalysts. By modification of the Pt with additional metals, CO-forming reactions were inhibited, resulting in high selectivity to C$_3$H$_6$. It was noted that the selectivity was not calculated on the basis of propane conversion and the formation of CO as a product from C$_3$H$_8$ was only considered in the Supporting Information.

Zhai et al. recently conducted a detailed mechanistic investigation into ODH−CO$_2$ using PtSn/SiO$_2$, highlighting the importance of the metal−metal oxide interface and showing that the RWGS reaction was rate-limiting.[70] The authors acknowledge the formation of CO from C$_3$H$_8$ via reforming and quantify this using the balance of CO observed as a proportion of CO$_2$ converted. However, the authors stop short of including CO as a product in the calculation of C$_3$H$_6$ selectivity, which makes it challenging to appreciate the contribution of reforming. Hence, supported NP catalysts are

among the most active catalysts reported for the activation of C_3H_8 and CO_2, but insufficient emphasis has been placed on understanding different reaction pathways in many of the studies published to date (Table 1). In this paper, we examine the importance of carbon monoxide formation during ODH−CO_2 over a series of catalysts that have been previously used for this reaction and have been well characterized and now concentrate on the structure−activity relationships that may influence C_3H_6 or CO formation. Experimentally, we revisit supported NPs and consider how reducible and nonreducible supports can influence different reaction pathways, using a robust method of reaction analysis, i.e., calculating selectivity based on converted C_3H_8 and specifically exploring the origin of CO as a reaction product. Additionally, we compare supported NP catalysts to commonly reported Ga_2O_3 and CrO_x/SiO_2 catalysts to determine whether reforming pathways are also prevalent on these catalysts. By considering a broad range of supports, we build a qualitative understanding of how different reaction pathways proceed over NP catalysts.

■ METHODS

Catalyst Preparation. γ-Al_2O_3, Ga_2O_3, $Ce(acac)_3$, Zr-$(acac)_4$, $Al(acac)_3$, and $Pd(NH_3)_4(NO_3)_2$ were obtained from Sigma-Aldrich, and ZrO_2 was obtained from Alfa Aesar. All chemicals and gases were research grade (99.9%+). SiO_2 (Davisil 62) was obtained from Davisil. Each compound was used without modification. $Ce_{0.5}Zr_{0.5}O_2$ and $Ce_{0.25}Zr_{0.25}Al_{0.5}O_x$ were prepared by physical grinding of acetylacetonate precursors of each metal, as previously described, which yielded an amorphous mixed metal oxide.[32] The salts were combined in a mortar and pestle, and the mixtures were ground for 10 min. Then, the powder was calcined in flowing air (300 °C, 2 h, 5 °C min^{-1}).

Supported Pd catalysts were prepared via wet impregnation. An appropriate quantity of $Pd(NO_3)_2(NH_3)_4$ was added to a 25 mL round-bottom flask with 2 cm^3 of deionized water, added to increase the volume of the solution above that of the pore volume of the supports. The support (0.950 g) was then added to the solution to form a slurry. The flask was placed in a silicon oil bath at 95 °C, and the solvent was left to evaporate overnight. The recovered powder was calcined in flowing air (500 °C, 5 °C min^{-1}, 4 h). CrO_x/SiO_2 was prepared in the same manner as the supported Pd catalysts, but $Cr(NO_3)_3$ was used instead. Ga_2O_3/Al_2O_3 was also prepared via wet impregnation of $Ga(NO_3)_3$ onto γ-Al_2O_3.

The supports for the series of Pt catalysts were prepared by the sol−gel method previously reported,[80,81] which yields nanocrystalline solid solutions of Ce and Zr oxides. Previous characterization of these solids indicated that the resultant phase for CeO_2, ZrO_2, and $Ce_{0.5}Zr_{0.5}O_2$ was cubic, tetragonal, and cubic, respectively. CeO_2, ZrO_2, and $Ce_{0.5}Zr_{0.5}O_2$ were formed in this way. Briefly, the metal precursor $(CeNO_3)_3 \cdot 6H_2O$ and/or $ZrO(NO_3) \cdot xH_2O$ (Sigma-Aldrich, 99.99%) were dissolved in deionized H_2O at 80 °C under vigorous stirring. NH_4OH (0.5 M, Fisher Scientific, 28−30 w/w% in H_2O) was added dropwise until the pH reached 9. The mixture was immediately filtered under vacuum and washed with warm distilled water before being dried (110 °C, 16 h) in a static oven. The resulting solid was ground using a mortar and pestle and calcined in flowing air (500 °C, 5 h, 10 °C min^{-1}).

Strong electrostatic adsorption (SEA) was used to prepare a series of 2 wt % Pt catalysts, in a similar manner to that previously reported.[82] Typically, 10 mL of NH_4OH (35 wt %)

was added to 50 mL of deionized water to form a solution of pH 12.5. The appropriate mass of $Pt(NH_3)_4Cl_2$ was dissolved in the solution, and then the support (1.94 g) was added with vigorous stirring. After 1 h, the mixture was filtered under vacuum, washed with deionized water (1 L), and dried in an oven for 16 h at 110 °C. The dried catalyst was reduced under flowing 5% H_2/Ar at 500, 600, 700, or 900 °C for 1 h. The same approach was used to prepare Pd/ZrO_2 catalysts using a pH of 13 to maximize the interaction of Pd and ZrO_2. 3 wt % Pt/SiO_2 was also prepared by this method, using aqueous tetraammine platinum hydroxide as the precursor.

Catalyst Testing. The catalysts were tested for ODH−CO_2 using a custom-made 16 parallel bed high-throughput reactor manufactured by Integrated Lab Solutions. The catalyst powders were pelleted and sieved to form 212−300 μm particles. Each catalyst (0.200 g) was diluted with SiC (typically 0.80 g) before being loaded into a quartz tube. The gas stream was analyzed via online gas chromatography.

Conversions and selectivity were calculated on the basis of moles of carbon converted (rather than observed products). The selectivity to CO was calculated in a similar manner to the hydrocarbon products but based on "excess CO" in the reaction. Excess CO is the observed CO in the reaction that cannot be formed from CO_2, i.e., it is formed from C_3H_8. Coke formation is inferred from the missing carbon in the quantification of products. This method is useful to compare relative tendencies for coke formation between catalysts but is limited where low levels of coke formation are observed. In this case, missing carbon could also be due to errors associated with GC analysis and quantification.

$$C_3H_8 \text{ Conversion (\%)} =$$
$$\frac{\text{moles propane in blank reactor bed} - \text{moles propane in reactor bed}}{\text{moles propane in blank reactor bed}}$$
$$\times 100\%$$

$$C_3H_6 \text{ Selectivity (\%)}$$
$$= \frac{\text{moles of propene observed} \times 3}{\text{moles of propane converted} \times 3} \times 100\%$$

$$CO \text{ Selectivity (\%)}$$
$$= \frac{\text{moles of CO} - \text{moles of } CO_2 \text{ converted}}{\text{moles of propane converted} \times 3} \times 100\%$$

$$\text{Converted carbon balance (\%)}$$
$$= \frac{\text{moles of carbon in observed products}}{\text{moles of carbon converted}} \times 100\%$$

Catalyst Characterization. Transmission electron microscopy (TEM) was carried out on a JEOL JEM-2100 operating at 200 kV. Aberration-corrected scanning transmission electron microscopy (AC-STEM) was carried out on a Spectra 200 scanning transmission electron microscope operating at 200 kV. All samples were prepared using a dry deposition method on a 300 mesh copper grid coated with a holey carbon film.

■ RESULTS AND DISCUSSION

The primary aim of this investigation was to understand how the catalyst support can influence the selectivity of the reaction toward C_3H_6 or CO. As CO is formed from the dissociation of CO_2, it must be distinguished from CO formed from C_3H_8 itself. This was achieved by considering the moles of excess

Table 2. Comparison of Commonly Reported ODH−CO₂ Catalysts[a]

| sample | time (h) | conversion (%) | | selectivity (%) | | | | | |
		C_3H_8	CO_2	CH_4	C_2H_4	C_2H_6	C_3H_6	CO	coke
Pd/CeZrAlO$_x$	1	31	66	3.6	0.2	0.4	10	33	53
	5	25	53	1.4	0.2	0.2	10	26	62
	9	20	45	1	0.2	0.2	12	32	55
β-Ga$_2$O$_3$	0.5	4.9	1.4	0.3	0.3	0.3	96	0	3
	4.5	2.8	1.0	0.2	0.4	0.6	75	0	24
	8.5	1.8	0.6	0.3	0.5	0.9	77	0	22
6 wt % CrO$_x$/SiO$_2$	1	11.2	6.1	2.5	0.7	0.6	96	0	0
	5	9.1	4.9	1.7	0.7	0.6	93	0	4
	9	7.6	3.9	1.5	0.8	0.7	96	0	1

[a]500 °C, 0.20 g catalyst + 0.80 g SiC (all catalysts pelleted to 200−300 μm), 10 vol % C_3H_8, 10 vol % CO_2, 80 vol % Ar, total flow rate = 10 mL min^{-1}, GHSV = ~3300 h^{-1}.
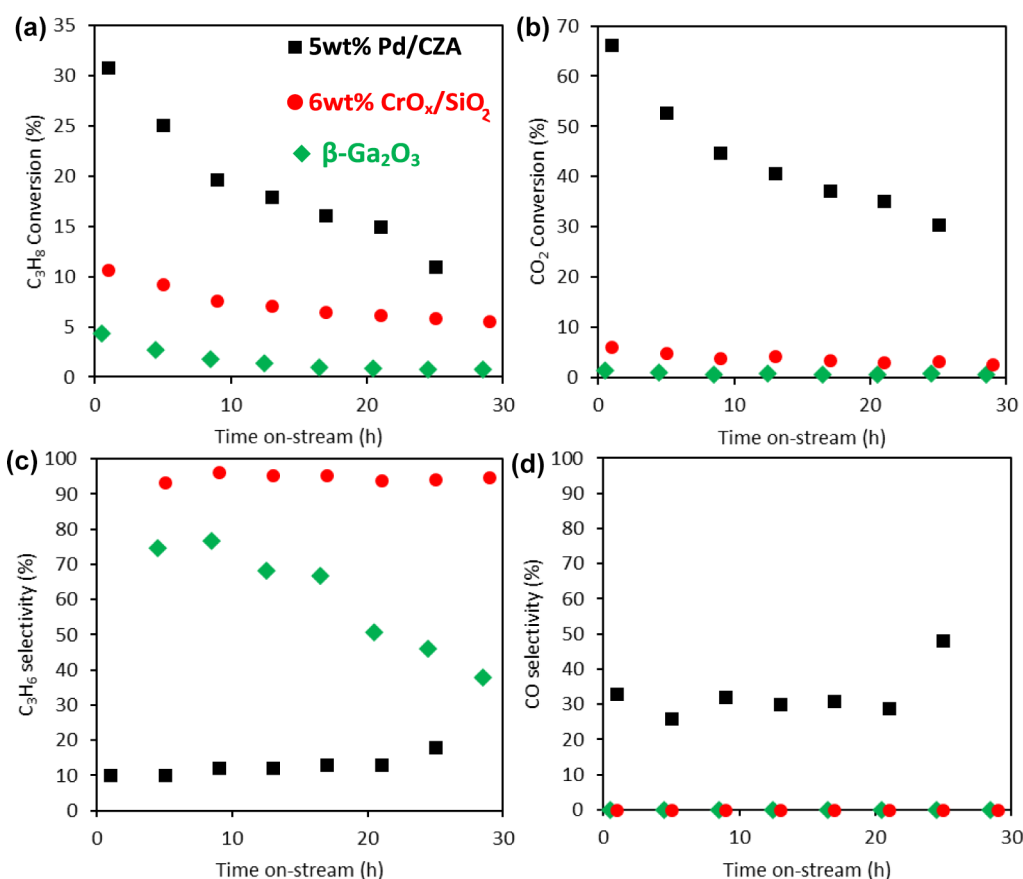
Figure 1. (a) C_3H_8 conversion, (b) CO_2 conversion, (c) C_3H_6 selectivity, and (d) CO selectivity of 5 wt % Pd/CZA, 6 wt % CrO_x/SiO$_2$, and β-Ga$_2$O$_3$.

CO observed as a proportion of the moles of carbon in propane that were converted in the reaction. Where the selectivity to CO from propane is 0%, there would be no excess CO measured; the moles of CO observed would be equal to the moles of CO_2 converted.

Using this approach, a series of commonly studied catalysts were prepared. 5 wt % Pd/CeZrAlO$_x$ was previously described by Nowicka et al.,[32] while Ga$_2$O$_3$ and 7 wt % CrO$_x$/SiO$_2$ represent two commonly investigated catalysts. Table 2 shows the activity of 5 wt % Pd/CeZrAlO$_x$, β-Ga$_2$O$_3$, and 7 wt % CrO$_x$/SiO$_2$.

Due to the nature of the sampling in the HTS reactor, the data obtained for different catalysts are not at the exact same time on-stream. Therefore, the performance of the catalysts is

best compared using time on-stream graphs, as shown in Figure 1a−d. 6 wt % CrO$_x$/SiO$_2$ exhibited an initial C_3H_8 and CO_2 conversion of around 10 and 5%, which decreased to ca. 7 and 4.2%, respectively, after 13 h on-stream. The selectivity for C_3H_6 was 93% initially, rising to 96% after 13 h on-stream. CH_4 was also observed as a minor product, and the missing carbon was attributed to coke deposition, in line with previous reports on CrO$_x$-based catalysts.[43,83,84] The Ga$_2$O$_3$ catalyst exhibited lower initial activity, with C_3H_8 and CO_2 conversions of 2.8 and 1.0%, respectively. The selectivity to C_3H_6 was 75%, and about 25% of converted carbon formed coke. It should be noted that at low C_3H_8 conversion (<5%), the error in measuring converted carbon becomes large and so the experimental error associated with measuring coke formation
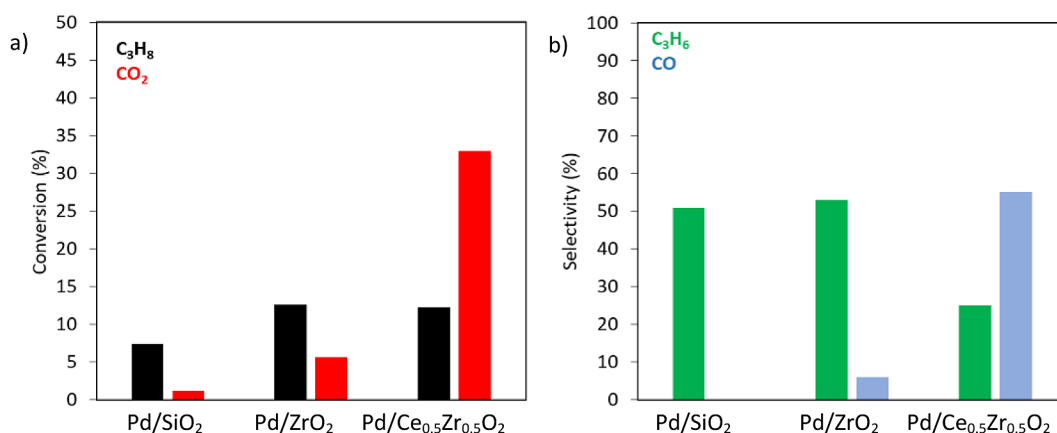
Figure 2. Comparison after 4 h on-stream of 5 wt % Pd/SiO_2, Pd/ZrO_2, and $Pd/Ce_{0.5}Zr_{0.5}O_2$ in the ODH−CO_2 reaction: (a) C_3H_8 and CO_2 conversion and (b) selectivity to C_3H_6 and CO. 500 °C, 0.20 g of catalyst + 0.80 g of SiC (200−300 μm), 10 vol % C_3H_8, 10 vol % CO_2, 80 vol % Ar, total flow: 10 mL min^{-1}, GHSV = ∼3300 h^{-1}. The bare supports were tested, and no conversion was observed (data not shown).
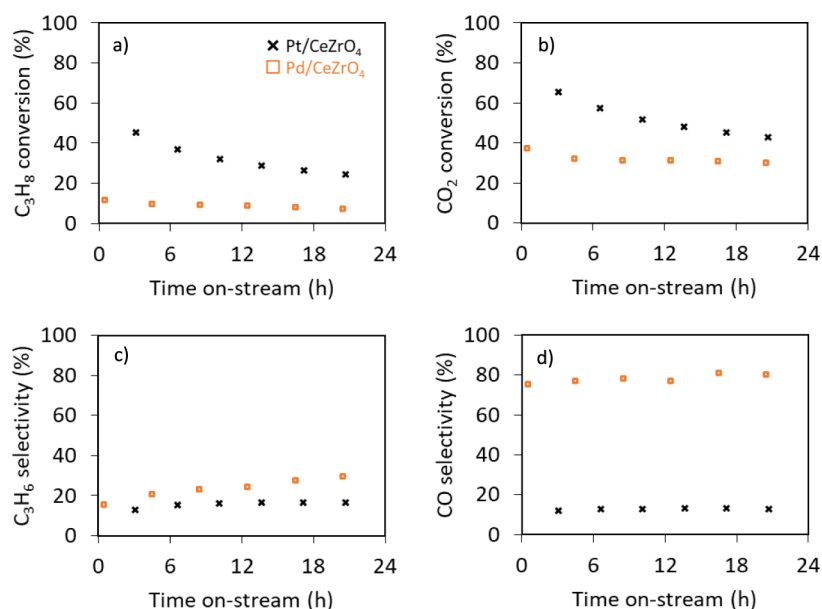

Figure 3. Comparison of 3 wt % $Pt/Ce_{0.5}Zr_{0.5}O_2$ and 5 wt % $Pd/Ce_{0.5}Zr_{0.5}O_2$ in the ODH−CO_2 reaction. (a) C_3H_8 conversion, (b) CO_2 conversion, (c) C_3H_6 selectivity, and (d) CO selectivity. 500 °C, 0.20 g catalyst + 0.80 g SiC (200−300 μm), 10 vol % C_3H_8, 10 vol % CO_2, 80 vol % Ar, total flow: 10 mL min^{-1}, GHSV = ∼3300 h^{-1}.

is greater. These two catalysts did not produce excess CO under these conditions, in contrast to $Pd/CeZrAlO_x$. The initial C_3H_8 and CO_2 conversion was 31 and 66%, respectively, and the selectivity to C_3H_6 and CO was 10 and 33%, respectively. CH_4 was also observed, but the majority of the remaining carbon was missing, i.e., converted to coke (ca. 53%). While the Pd/CZA catalyst was the most active, clearly, there were significant CO-forming side-reactions occurring. These could be dry/steam reforming or the reverse Boudouard reaction. In the cases of CrO_x/SiO_2 and Ga_2O_3, the conversion of C_3H_8 is higher than that of CO_2, even when the contribution to coke is considered. This means that there must be additional reactions occurring beyond the ODH−CO_2 reaction (eq 1 or eqs 2 and 3); specifically, DDH and some cracking/methanation reactions took place.

On the basis of the above data, it is clear that CrO_x and Ga_2O_3 catalysts do not catalyze CO-forming reactions, whereas $Pd/CeZrAlO_x$ does. The origin of high CO selectivity was

investigated by considering the role of the support in determining the balance of different reaction pathways. 5 wt % Pd supported on SiO_2 (Davisil grade 62), ZrO_2, and $Ce_{0.5}Zr_{0.5}O_2$ were subsequently prepared via wet impregnation, and the reaction data are shown in Figure 2.

The supports can be categorized into nonreducible (SiO_2), poorly reducible (ZrO_2), and highly reducible ($Ce_{0.5}Zr_{0.5}O_2$). 5 wt % Pd/SiO_2 exhibited low conversion of C_3H_8 and almost no CO_2 conversion (7.4 and 1.2%, respectively), but with 51% selectivity to C_3H_6, 48% selectivity to coke, and trace amounts of cracked products (<1%). Significantly, no excess CO was observed. 5 wt % Pd/ZrO_2 exhibited an improved C_3H_8 and CO_2 conversion of 12.6 and 5.6%, respectively, but resulted in 6% selectivity to CO. The selectivity to C_3H_6 was very similar at 53%, while the selectivity to coke was slightly lower than 5 wt % Pd/SiO_2 at 40%. 5 wt % $Pd/Ce_{0.5}Zr_{0.5}O_2$ exhibited a similar C_3H_8 conversion (12.2%) but a significantly increased CO_2 conversion of 33%. This corresponded to a sharp rise in
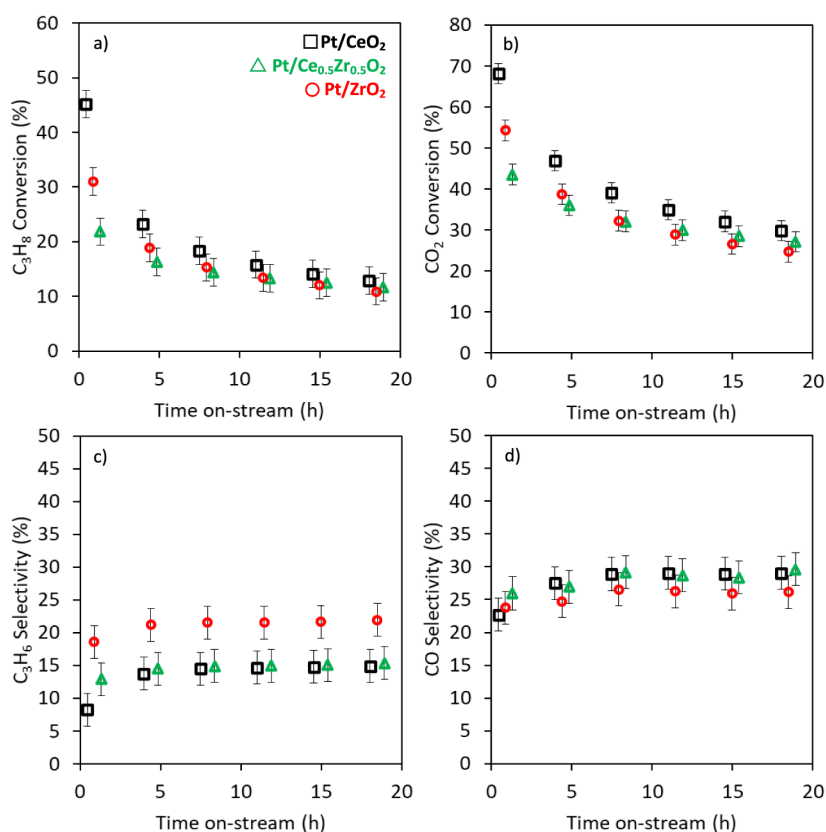
Figure 4. Comparison of supported Pt catalysts with comparable Pt particle sizes. (a) C_3H_8 conversion, (b) CO_2 conversion, (c) C_3H_6 selectivity, and (d) CO selectivity, where □ = Pt/CeO$_2$, △ = Pt/Ce$_{0.5}$Zr$_{0.5}$O$_2$, and ○ = Pt/ZrO$_2$.

CO selectivity (55%) and a lower selectivity to C_3H_6 of 25%. The trends in these data reveal that the reducibility of the support is a major factor in determining C_3H_8 conversion and selectivity to C_3H_6 or CO: Pd nanoparticles supported on reducible supports are highly active but promote undesirable CO-forming reactions.

Platinum is one of the most studied metals for DDH and is the active component in three commercialized processes, namely Oleflex, Dow FCdh, and Uhde STAR processes.[12] Therefore, it is of interest to study this metal in the context of ODH−CO$_2$ to understand if the selectivity toward CO is influenced by the choice of supported metal. 3 wt % Pt was chosen as the metal loading as it balances a high concentration of active metal phase with the ability to prepare small, well-dispersed nanoparticles. SiO$_2$ and Ce$_{0.5}$Zr$_{0.5}$O$_2$ were selected to contrast the performance of a highly reducible support (Ce$_{0.5}$Zr$_{0.5}$O$_2$) with a nonreducible support (SiO$_2$). 3% Pt/SiO$_2$ exhibited very low conversion (<2%) of both C_3H_8 and CO$_2$, consistent with the 5% Pd/SiO$_2$ catalyst above and in-line with control reactions without a catalyst present. This inactivity indicates that an appropriate support is necessary to realize high activity in supported metal NPs. The performance of Pd/Ce$_{0.5}$Zr$_{0.5}$O$_2$ and Pt/Ce$_{0.5}$Zr$_{0.5}$O$_2$ is shown in Figure 3. Pt/Ce$_{0.5}$Zr$_{0.5}$O$_2$ exhibited very high initial conversion of C_3H_8 and CO$_2$ (45 and 66%, respectively). The selectivity to C_3H_6 and CO was 13 and 12%, respectively. Ca. 60% of the carbon was unaccounted for, indicating prevalent coke formation, and CH$_4$, C$_2$H$_4$, and C$_2$H$_6$ selectivity was 10, 5.6, and 1.3%, respectively. The C$_1$ and C$_2$ products observed in the Pd/Ce$_{0.5}$Zr$_{0.5}$O$_2$ catalyst accounted for ca. 1% selectivity, indicating that cracking reactions are more prevalent over Pt/

Ce$_{0.5}$Zr$_{0.5}$O$_2$, although the difference in selectivity may have been due to increased C_3H_8 conversion.

The main differences between the Pt/Ce$_{0.5}$Zr$_{0.5}$O$_2$ and Pd/Ce$_{0.5}$Zr$_{0.5}$O$_2$ catalysts were that Pt was more active and less selective to CO but favored coke formation. Pd/Ce$_{0.5}$Zr$_{0.5}$O$_2$ was less active than Pt and favored CO-forming reactions. The overall conclusion of this comparison is that the supported metal and the support both determine the dominant reaction pathways. An important facet of this is NP size, and it should be acknowledged that the difference in NP size of the Pd and Pt catalysts above would impact the catalyst performance. Indeed, there are various reports that demonstrate that the size of Pt NPs affects the catalytic performance of DDH catalysts, and similar trends may be expected in ODH−CO$_2$. The purpose of the comparisons above is to illustrate the sensitivity of the catalyst to the nature of the supported metal, rather than the activity being determined by the support composition only.

To carefully probe the effect of NP size, 2 wt % Pt supported on CeO$_2$, ZrO$_2$, and Ce$_{0.5}$Zr$_{0.5}$O$_2$ were prepared via strong-electrostatic adsorption to produce a set of samples with similar particle sizes and different support characteristics. TEM was carried out to measure the particle sizes, and these data are shown in Figure S1. The images and particle size distribution revealed that the as-prepared Pt nanoparticles were similar in size (all samples showed an average Pt particle size of 1.2−1.5 nm after reduction) and therefore any observed differences in catalytic activity may be traced to the properties of the support. Figure 4 shows the activity of the catalysts in the presence of ODH−CO$_2$.

The data in Figure 4 show that when Pt particle size is controlled, the difference in performance is rather small. The
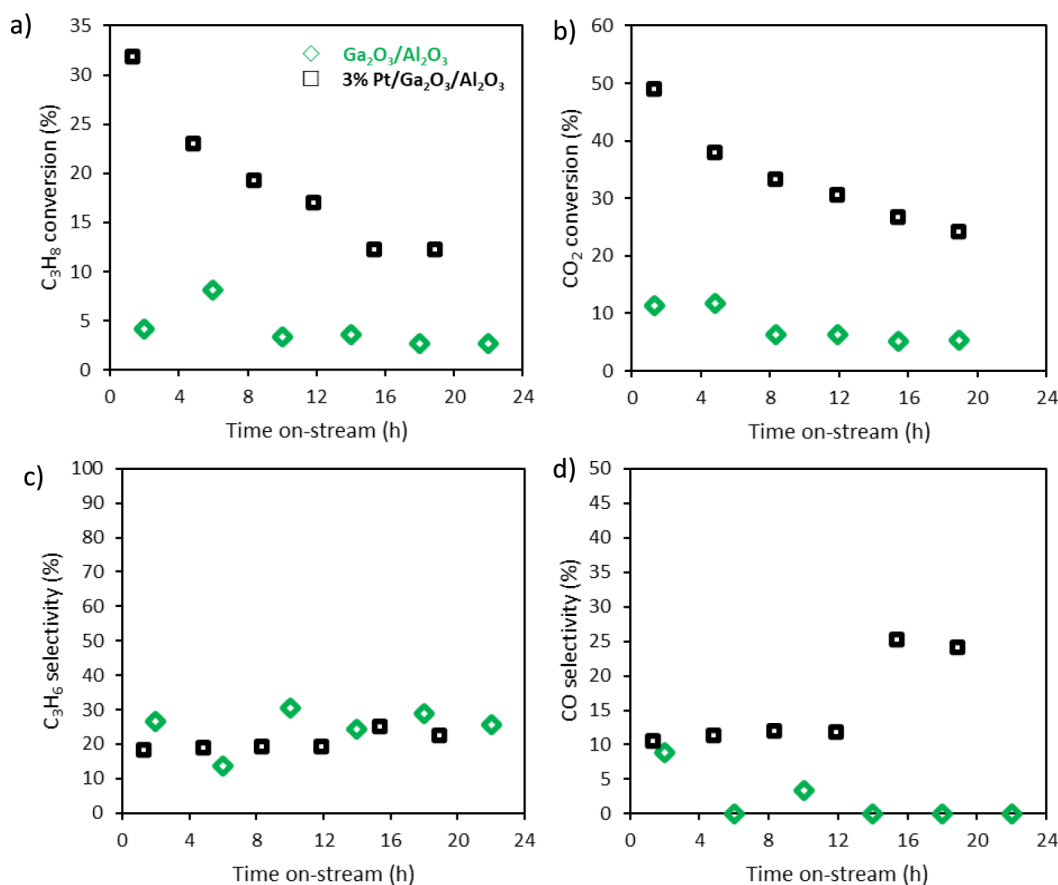
Figure 5. Comparison of Ga_2O_3/Al_2O_3 (green diamonds) and 3 wt % $Pt/Ga_2O_3/Al_2O_3$ (black squares) in the ODH–CO_2 reaction: (a) C_3H_8 conversion, (b) CO_2 conversion, (c) C_3H_6 selectivity, and (d) CO selectivity (500 °C, 10 vol % C_3H_8, 10 vol % CO_2, N_2, and Ar to balance). Total flow rate = 10 mL min^{-1}, 0.20 g of catalyst.

steady-state conversion of C_3H_8 and CO_2 for all catalysts is the same within experimental error, while the Pt/ZrO_2 catalyst exhibited a higher C_3H_6 selectivity than those containing CeO_2. The origin of this difference in selectivity is unclear, but it has been shown that the metal–support interface plays a crucial role in determining reaction pathways in the ODH–CO_2: Zhai et al. recently reported detailed kinetic and mechanistic investigations into $Pt–Sn/SiO_2$ catalysts for ODH–CO_2.[70] The authors concluded that the reaction proceeded via a two-step reaction mechanism, where DDH is followed by RWGS, and that specific Pt ensembles are responsible for C–H or C–C cleavage. It is possible that the Pt NP shape or faceting in the Pt/ZrO_2 catalyst inhibits C–C cleavage compared to the other supports, but this requires further investigation. The performance of supported Pd catalysts showed the presence of Ce in the support resulted in higher CO formation; however, the differences for the Pt catalysts are more subtle than in the Pd catalysts: similar CO formation was observed across each of the Pt catalysts. These data confirm that both the support and the supported metal composition and structure play a role in favoring CO or C_3H_6 formation.

The data presented above show that mixed metal oxide catalysts such as gallia and vanadia do not promote CO formation but can form C_3H_6 with moderate activity. Pt, meanwhile, exhibits high activity but poor selectivity to C_3H_6. Therefore, $Pt/Ga_2O_3/Al_2O_3$ was identified as a promising candidate to investigate further. The presence of Al_2O_3 offers a

thermally stable support to host Pt and Ga. Pt was deposited on 5 wt % Ga_2O_3/Al_2O_3 via SEA in order to assess the effect of Pt addition on the selectivity to excess CO. The results are shown in Figure 5. In the absence of Pt, the Ga_2O_3/Al_2O_3 catalyst exhibited low conversion (~5%), moderate selectivity to C_3H_6 (~25–30%), and no selectivity to CO (0% after 10 h on-stream). The addition of Pt caused a considerable increase in the initial conversion of C_3H_8 and CO_2 to 30 and 50%, respectively. The selectivity for C_3H_8 was similar (~25%), but the CO selectivity was increased (10–25%). These data clearly show that Pt can promote CO formation without a reducible oxide present and further demonstrate that both the support functionality and the supported metal contribute to catalyst performance. Careful consideration should be given to the composition and interplay of both of these catalyst components.

Although excess CO formation was confirmed over various supported NP catalysts, the origin of formation has not been investigated. As discussed above, there are various possible reactions that could produce excess CO in this reaction, namely, dry reforming, steam reforming, and the reverse Boudouard reaction. However, it is not apparent if some or all of these reactions take place under reaction conditions. Xing et al. demonstrated that the reverse Boudouard reaction can readily occur at 550 °C over $Pt–In–Co/CeO_2$ catalysts.[79] The lower temperature reaction may mean that in the current work, CO formation from coke is less prevalent. Steam reforming has not been experimentally demonstrated in the context of the

oxidation of ODH−CO$_2$. As H$_2$O is required in this reaction, steam reforming would be expected to occur under high C$_3$H$_8$ conversion. To investigate steam reforming experimentally, C$_3$H$_8$ and H$_2$O were cofed over a Pd/Ce$_{0.5}$Zr$_{0.5}$O$_2$ catalyst. The conditions were selected to replicate the stoichiometric requirements and demonstrate the feasibility of the reaction at 500 °C. Figure S2 shows the concentration of the reactants and products, and the data clearly show that this catalyst can catalyze steam reforming at 500 °C. Overall, steam reforming should be considered as a significant contributing reaction pathway, especially at higher C$_3$H$_8$ conversions where the partial pressure of H$_2$O will be higher.

CONCLUSIONS

Many of the previous studies into ODH−CO$_2$ have overlooked CO as a reaction product of C$_3$H$_8$.[32] The results of the current study show that CO is readily formed over supported NPs and could originate from various pathways, especially reforming. The data presented in this paper illustrate that the structure−activity relationships that govern the selectivity of the reaction are complex. On one hand, Pd or Pt NPs supported on cerium oxide-based supports catalyze CO formation as much as, or more than, C$_3$H$_6$ formation. However, in the absence of a reducible support, the catalytic activity is very poor, indicating that an additional functionality is necessary, i.e., in the form of an active support. Commonly reported catalysts, e.g., CrO$_x$/SiO$_2$ and Ga$_2$O$_3$−Al$_2$O$_3$ do not catalyze CO formation but are intrinsically less active than NP-based catalysts. When Pt was supported on Ga$_2$O$_3$−Al$_2$O$_3$, the activity was greatly increased, but with the increased formation of CO. In general, the performance of ODH−CO$_2$ catalysts was hindered by low activity or poor selectivity to C$_3$H$_6$, as is the case with supported NP particles.

As discussed in the introduction, many literature reports do not calculate C$_3$H$_6$ on the basis of converted C$_3$H$_8$, which leaves open the possibility of inflated selectivity calculations. The current work has shown that the formation of CO is not prevalent on Cr- and Ga-based catalysts, whereas over NP catalysts, the potential for CO production from C$_3$H$_8$ is much greater. Therefore, special attention should be paid to research reports where supported NPs are investigated and selectivity is *not* calculated using converted C$_3$H$_8$. Consideration of the chronology of this field of catalysis may help to explain why the majority of the literature on this reaction does not consider CO as a potential reaction product. The early studies were based on Ga-, Cr- and other mixed metal oxide catalysts and were conducted using conditions similar to conventional nonoxidative C$_3$H$_8$ dehydrogenation. With these catalysts and conditions, CO formation does not occur, and therefore, close scrutiny of the products formed was not considered to be required. However, the recent interest in NP catalysts demands the most robust analytical approaches to accurately quantify the products of the reaction.

Future research should focus on harnessing the high activity of supported NP catalysts while inhibiting the deleterious pathways that produce CO. Such breakthroughs have been made where noble metals supported on CeO$_2$ were modified with transition metals, e.g., Fe, In, and Co.[78,79] The nanostructure of these catalysts is highly complex, but the step-change in performance should incentivize further investigation into similar catalyst formulations. Finally, further experiments are required to quantify the structure−activity relationships present in these catalysts.

ASSOCIATED CONTENT

ⓈI Supporting Information

The Supporting Information is available free of charge at https://pubs.acs.org/doi/10.1021/acscatal.4c02628.

BF-TEM images of catalysts (Figure S1); time on stream catalysis analysis data (Figure S2) (PDF)

AUTHOR INFORMATION

Corresponding Authors

James H. Carter − *Max Planck-Cardiff Centre on the Fundamentals of Heterogeneous Catalysis FUNCAT, Cardiff Catalysis Institute, School of Chemistry, Cardiff University, Translational Research Hub, Cardiff University, Cardiff CF24 4HQ, U.K.*; Email: carterj5@cf.ac.uk

Graham J. Hutchings − *Max Planck-Cardiff Centre on the Fundamentals of Heterogeneous Catalysis FUNCAT, Cardiff Catalysis Institute, School of Chemistry, Cardiff University, Translational Research Hub, Cardiff University, Cardiff CF24 4HQ, U.K.*; orcid.org/0000-0001-8885-1560; Email: hutch@cf.ac.uk

Authors

Tongqi Ye − *School of Chemistry and Chemical Engineering, Hefei University of Technology, Hefei, Anhui 230009, PR China*

Daniel G. Hewes − *Max Planck-Cardiff Centre on the Fundamentals of Heterogeneous Catalysis FUNCAT, Cardiff Catalysis Institute, School of Chemistry, Cardiff University, Translational Research Hub, Cardiff University, Cardiff CF24 4HQ, U.K.*

Ahlam Almoteiry − *Max Planck-Cardiff Centre on the Fundamentals of Heterogeneous Catalysis FUNCAT, Cardiff Catalysis Institute, School of Chemistry, Cardiff University, Translational Research Hub, Cardiff University, Cardiff CF24 4HQ, U.K.*

Kieran J. Aggett − *Max Planck-Cardiff Centre on the Fundamentals of Heterogeneous Catalysis FUNCAT, Cardiff Catalysis Institute, School of Chemistry, Cardiff University, Translational Research Hub, Cardiff University, Cardiff CF24 4HQ, U.K.*

Bart D. Vandegehuchte − *TotalEnergies OneTech Belgium, Seneffe B-7181, Belgium*

Christopher J. Kiely − *Department of Materials Science and Engineering, Lehigh University, Bethlehem, Pennsylvania 18015, United States*

Stuart H. Taylor − *Max Planck-Cardiff Centre on the Fundamentals of Heterogeneous Catalysis FUNCAT, Cardiff Catalysis Institute, School of Chemistry, Cardiff University, Translational Research Hub, Cardiff University, Cardiff CF24 4HQ, U.K.*; orcid.org/0000-0002-1933-4874

Complete contact information is available at:
https://pubs.acs.org/10.1021/acscatal.4c02628

Notes

The authors declare no competing financial interest.

■ REFERENCES

(1) Chen, S.; Chang, X.; Sun, G.; Zhang, T.; Xu, Y.; Wang, Y.; Pei, C.; Gong, J. Propane Dehydrogenation: Catalyst Development, New Chemistry, and Emerging Technologies. *Chem. Soc. Rev.* **2021**, *50* (5), 3315−3354.

(2) Santhosh Kumar, M.; Hammer, N.; Rønning, M.; Holmen, A.; Chen, D.; Walmsley, J. C.; Øye, G. The Nature of Active Chromium Species in Cr-Catalysts for Dehydrogenation of Propane: New Insights by a Comprehensive Spectroscopic Study. *J. Catal.* **2009**, *261* (1), 116−128.

(3) Hydrocarbon Engineering. *KBR signs agreement for propane dehydrogenation project.* https://www.hydrocarbonengineering.com/petrochemicals/14042021/kbr-signs-agreement-for-propane-dehydrogenation-project/ (accessed 06 May 2021).

(4) Kogan, S. B.; Herskowitz, M. Selective Propane Dehydrogenation to Propylene on Novel Bimetallic Catalysts. *Catal. Commun.* **2001**, *2* (5), 179−185.

(5) Global Data. Global Propylene Capacity and Capital Expenditure Outlook to 2030 − Asia and Middle East to Lead Globally in Terms of Propylene Capacity Additions; 2021. https://store.globaldata.com/report/gdch0067mar--global-propylene-capacity-and-capital-expenditure-outlook-to-2030-asia-and-middle-east-to-lead-globally-in-terms-of-propylene-capacity-additions/ (accessed 2021−05−04).

(6) Zhang, T.; Pei, C.; Sun, G.; Chen, S.; Zhao, Z.; Sun, S.; Lu, Z.; Xu, Y.; Gong, J. Synergistic Mechanism of Platinum-GaO$_x$ Catalysts for Propane Dehydrogenation. *Angew. Chem.* **2022**, *134* (35), 61−68.

(7) Santhosh Kumar, M.; Chen, D.; Holmen, A.; Walmsley, J. C. Dehydrogenation of Propane over Pt-SBA-15 and Pt-Sn-SBA-15: Effect of Sn on the Dispersion of Pt and Catalytic Behavior. *Catal. Today* **2009**, *142* (1−2), 17−23.

(8) Kaylor, N.; Davis, R. J. Propane Dehydrogenation over Supported Pt-Sn Nanoparticles. *J. Catal.* **2018**, *367*, 181−193.

(9) De Rossi, S.; Ferraris, G.; Fremiotti, S.; Garrone, E.; Ghiotti, G.; Campa, M. C.; Indovina, V. Propane Dehydrogenation on Chromia/Silica and Chromia/Alumina Catalysts. *J. Catal.* **1994**, *148*, 36−46.

(10) Puurunen, R. L.; Weckhuysen, B. M. Spectroscopic Study on the Irreversible Deactivation of Chromia/Alumina Dehydrogenation Catalysts. *J. Catal.* **2002**, *210* (2), 418−430.

(11) UK Deptartment of Energy & Climate Change; Atlantic Consulting; Menecon Consulting. *RHI Evidence Report: biopropane For Grid Injection*, 2014. https://assets.publishing.service.gov.uk/government/uploads/system/uploads/attachment_data/file/376487/RHI_Evidence_Report_-_Biopropane_for_Grid_Injection__2____2_.pdf.

(12) Carter, J. H.; Bere, T.; Pitchers, J. R.; Hewes, D. G.; Vandegehuchte, B. D.; Kiely, C. J.; Taylor, S. H.; Hutchings, G. J. Direct and Oxidative Dehydrogenation of Propane: From Catalyst Design to Industrial Application. *Green Chem.* **2021**, *23* (24), 9747−9799.

(13) Jablonski, E. L.; Castro, A. A.; Scelza, O. A.; De Miguel, S. R. Effect of Ga Addition to Pt/Al2O3 on the Activity, Selectivity and Deactivation in the Propane Dehydrogenation. *Appl. Catal. A Gen.* **1999**, *183* (1), 189−198.

(14) Sokolov, S.; Stoyanova, M.; Rodemerck, U.; Linke, D.; Kondratenko, E. V. Comparative Study of Propane Dehydrogenation over V-, Cr-, and Pt-Based Catalysts: Time on-Stream Behavior and Origins of Deactivation. *J. Catal.* **2012**, *293*, 67−75.

(15) Venegas, J. M.; Zhang, Z.; Agbi, T. O.; McDermott, W. P.; Alexandrova, A.; Hermans, I. Why Boron Nitride Is Such a Selective Catalyst for the Oxidative Dehydrogenation of Propane. *Angew. Chem., Int. Ed.* **2020**, *59* (38), 16527−16535.

(16) Lu, W. D.; Wang, D.; Zhao, Z.; Song, W.; Li, W. C.; Lu, A. H. Supported Boron Oxide Catalysts for Selective and Lowerature Oxidative Dehydrogenation of Propane. *ACS Catal.* **2019**, *9* (9), 8263−8270.

(17) Shi, L.; Wang, D.; Lu, A. H. A Viewpoint on Catalytic Origin of Boron Nitride in Oxidative Dehydrogenation of Light Alkanes. *Chin. J. Catal.* **2018**, *39* (5), 908−913.

(18) Zhang, X.; You, R.; Wei, Z.; Jiang, X.; Yang, J.; Pan, Y.; Wu, P.; Jia, Q.; Bao, Z.; Bai, L.; Jin, M.; Sumpter, B.; Fung, V.; Huang, W.; Wu, Z. Radical Chemistry and Reaction Mechanisms of Propane Oxidative Dehydrogenation over Hexagonal Boron Nitride Catalysts. *Angew. Chem., Int. Ed.* **2020**, *59* (21), 8042−8046.

(19) Shi, L.; Wang, Y.; Yan, B.; Song, W.; Shao, D.; Lu, A. H. Progress in Selective Oxidative Dehydrogenation of Light Alkanes to Olefins Promoted by Boron Nitride Catalysts. *Chem. Commun.* **2018**, *54* (78), 10936−10946.

(20) Takahara, I.; Saito, M. Promoting Effects of Carbon Dioxide on Dehydrogenation of Propane over a SiO2-Supported Cr2O3 Catalyst. *Chem. Lett.* **1996**, *25* (11), 973−974.

(21) Michorczyk, P.; Zeńczak-Tomera, K.; Michorczyk, B.; Węgrzyniak, A.; Basta, M.; Millot, Y.; Valentin, L.; Dzwigaj, S. Effect of Dealumination on the Catalytic Performance of Cr-Containing Beta Zeolite in Carbon Dioxide Assisted Propane Dehydrogenation. *J. CO2 Util.* **2020**, *36*, 54−63.

(22) Nakagawa, K.; Okamura, M.; Ikenaga, N.; Suzuki, T.; Kobayashi, T. Dehydrogenation of Ethane over Gallium Oxide in the Presence of Carbon Dioxide. *Chem. Commun.* **1998**, No. 9, 1025−1026.

(23) Michorczyk, P.; Ogonowski, J.; Kuśtrowski, P.; Chmielarz, L. Chromium Oxide Supported on MCM-41 as a Highly Active and Selective Catalyst for Dehydrogenation of Propane with CO2. *Appl. Catal. A Gen.* **2008**, *349* (1−2), 62−69.

(24) Michorczyk, P.; Pietrzyk, P.; Ogonowski, J. Preparation and Characterization of SBA-1-Supported Chromium Oxide Catalysts for CO 2 Assisted Dehydrogenation of Propane. *Microporous Mesoporous Mater.* **2012**, *161*, 56−66.

(25) Chen, M.; Xu, J.; Liu, Y. M.; Cao, Y.; He, H. Y.; Zhuang, J. H.; Fan, K. N. Enhanced Activity of Spinel-Type Ga2O3-Al 2O3Mixed Oxide for the Dehydrogenation of Propane in the Presence of CO2. *Catal. Lett.* **2008**, *124* (3−4), 369−375.

(26) Chen, M.; Xu, J.; Su, F. Z.; Liu, Y. M.; Cao, Y.; He, H. Y.; Fan, K. N. Dehydrogenation of Propane over Spinel-Type Gallia-Alumina Solid Solution Catalysts. *J. Catal.* **2008**, *256* (2), 293−300.

(27) Tian, H.; Liao, J.; Zha, F.; Guo, X.; Tang, X.; Chang, Y.; Ma, X. Catalytic Performance of In/HZSM-5 for Coupling Propane with CO2 to Propylene. *ChemistrySelect* **2020**, *5* (12), 3626−3637.

(28) Chen, M.; Wu, J. L.; Liu, Y. M.; Cao, Y.; Guo, L.; He, H. Y.; Fan, K. N. Study in Support Effect of In2O3/MOx (M = Al, Si, Zr) Catalysts for Dehydrogenation of Propane in the Presence of CO 2. *Appl. Catal. A Gen.* **2011**, *407* (1−2), 20−28.

(29) Han, Z. F.; Xue, X. L.; Wu, J. M.; Lang, W. Z.; Guo, Y. J. Preparation and Catalytic Properties of Mesoporous NV-MCM-41 for Propane Oxidative Dehydrogenation in the Presence of CO 2. *Chin. J. Catal.* **2018**, *39* (6), 1099−1109.

(30) Michorczyk, P.; Kuśtrowski, P.; Chmielarz, L.; Ogonowski, J. Influence of Redox Properties on the Activity of Iron Oxide Catalysts in Dehydrogenation of Propane with CO2. *React. Kinet. Catal. Lett.* **2004**, *82* (1), 121−130.

(31) Ren, Y.; Zhang, F.; Hua, W.; Yue, Y.; Gao, Z. ZnO Supported on High Silica HZSM-5 as New Catalysts for Dehydrogenation of Propane to Propene in the Presence of CO2. *Catal. Today* **2009**, *148* (3−4), 316−322.

(32) Nowicka, E.; Reece, C.; Althahban, S. M.; Mohammed, K. M. H.; Kondrat, S. A.; Morgan, D. J.; He, Q.; Willock, D. J.; Golunski, S.; Kiely, C. J.; et al. Elucidating the Role of CO2 in the Soft Oxidative Dehydrogenation of Propane over Ceria-Based Catalysts. *ACS Catal.* **2018**, *8* (4), 3454−3468.

(33) Sullivan, M. M.; Bhan, A. Effects of Oxygen Coverage on Rates and Selectivity of Propane-CO2 Reactions on Molybdenum Carbide. *J. Catal.* **2018**, *357*, 195−205.

(34) Yun, D.; Baek, J.; Choi, Y.; Kim, W.; Lee, H. J.; Yi, J. Promotional Effect of Ni on a CrOx Catalyst Supported on Silica in the Oxidative Dehydrogenation of Propane with CO2. *ChemCatchem* **2012**, *4* (12), 1952−1959.

(35) Du, X.; Yao, B.; Gonzalez-Cortes, S.; Kuznetsov, V. L.; Almegren, H.; Xiao, T.; Edwards, P. P. Catalytic Dehydrogenation of Propane by Carbon Dioxide: A Medium-Temperature Thermochemical Process for Carbon Dioxide Utilisation. *Faraday Discuss.* **2015**, *183*, 161−176.

(36) Kuśtrowski, P.; Michorczyk, P.; Chmielarz, L.; Piwowarska, Z.; Dudek, B.; Ogonowski, J.; Dziembaj, R. TG Study on Real Role of Active Carbon Support in Propane Dehydrogenation with CO2. *Thermochim. Acta* **2008**, *471* (1−2), 26−32.

(37) Wang, H. M.; Chen, Y.; Yan, X.; Lang, W. Z.; Guo, Y. J. Cr Doped Mesoporous Silica Spheres for Propane Dehydrogenation in the Presence of CO2: Effect of Cr Adding Time in Sol-Gel Process. *Microporous Mesoporous Mater.* **2019**, *284*, 69−77.

(38) Botavina, M. A.; Agafonov, Y. A.; Gaidai, N. A.; Groppo, E.; Lapidus, A. L.; Martra, G. Towards Efficient Catalysts for the Oxidative Dehydrogenation of Propane in the Presence of CO2: Cr/SiO2 Systems Prepared by Direct Hydrothermal Synthesis. *Catal. Sci. Technol.* **2016**, *6* (3), 840−850.

(39) de Oliveira, J. F. S.; Volanti, D. P.; Bueno, J. M. C.; Ferreira, A. P. Effect of CO2 in the Oxidative Dehydrogenation Reaction of Propane over Cr/ZrO2 Catalysts. *Appl. Catal. A Gen.* **2018**, *558*, 55−66.

(40) Zhang, F.; Wu, R.; Yue, Y.; Yang, W.; Gu, S.; Miao, C.; Hua, W.; Gao, Z. Chromium Oxide Supported on ZSM-5 as a Novel Efficient Catalyst for Dehydrogenation of Propane with CO2. *Microporous Mesoporous Mater.* **2011**, *145* (1−3), 194−199.

(41) Michorczyk, P.; Ogonowski, J.; Zeńczak, K. Activity of Chromium Oxide Deposited on Different Silica Supports in the Dehydrogenation of Propane with CO2 - A Comparative Study. *J. Mol. Catal. A: Chem.* **2011**, *349* (1−2), 1−12.

(42) Wu, R.; Xie, P.; Cheng, Y.; Yue, Y.; Gu, S.; Yang, W.; Miao, C.; Hua, W.; Gao, Z. Hydrothermally Prepared Cr2O3-ZrO2 as a Novel Efficient Catalyst for Dehydrogenation of Propane with CO2. *Catal. Commun.* **2013**, *39*, 20−23.

(43) Baek, J.; Yun, H. J.; Yun, D.; Choi, Y.; Yi, J. Preparation of Highly Dispersed Chromium Oxide Catalysts Supported on Mesoporous Silica for the Oxidative Dehydrogenation of Propane Using CO 2: Insight into the Nature of Catalytically Active Chromium Sites. *ACS Catal.* **2012**, *2* (9), 1893−1903.

(44) Michorczyk, P.; Ogonowski, J.; Niemczyk, M. Investigation of Catalytic Activity of CrSBA-1 Materials Obtained by Direct Method in the Dehydrogenation of Propane with CO2. *Appl. Catal. A Gen.* **2010**, *374* (1−2), 142−149.

(45) Zhang, X.; Yue, Y.; Gao, Z. Chromium Oxide Supported on Mesoporous SBA-15 as Propane Dehydrogenation and Oxidative Dehydrogenation Catalysts. *Catal. Lett.* **2002**, *83* (1−2), 19−25.

(46) Zhu, Q.; Takiguchi, M.; Setoyama, T.; Yokoi, T.; Kondo, J. N.; Tatsumi, T. Oxidative Dehydrogenation of Propane with CO2 over Cr/H[B]MFI Catalysts. *Catal. Lett.* **2011**, *141* (5), 670−677.

(47) Li, L.; Zhu, W.; Shi, L.; Liu, Y.; Liu, H.; Ni, Y.; Liu, S.; Zhou, H.; Liu, Z. The Effect of Ethanol on the Performance of CrOx/SiO2 Catalysts during Propane Dehydrogenation. *Chin. J. Catal.* **2016**, *37* (3), 359−366.

(48) Michorczyk, P.; Ogonowski, J. Simultaneous Propane Dehydrogenation and CO2 Hydrogenation over CrOx/SiO2 Catalyst. *React. Kinet. Catal. Lett.* **2005**, *87* (1), 177−183.

(49) Xie, Z.; Ren, Y.; Li, J.; Zhao, Z.; Fan, X.; Liu, B.; Song, W.; Kong, L.; Xiao, X.; Liu, J.; et al. Facile in Situ Synthesis of Highly Dispersed Chromium Oxide Incorporated into Mesoporous ZrO2 for the Dehydrogenation of Propane with CO2. *J. Catal.* **2019**, *372*, 206−216.

(50) Takehira, K.; Ohishi, Y.; Shishido, T.; Kawabata, T.; Takaki, K.; Zhang, Q.; Wang, Y. Behavior of Active Sites on Cr-MCM-41 Catalysts during the Dehydrogenation of Propane with CO2. *J. Catal.* **2004**, *224* (2), 404−416.

(51) Jin, R.; Easa, J.; Tran, D. T.; O'Brien, C. P. Ru-Promoted CO2 Activation for Oxidative Dehydrogenation of Propane over Chromium Oxide Catalyst. *Catal. Sci. Technol.* **2020**, *10* (6), 1769−1777.

(52) Dou, J.; Funderburg, J.; Yang, K.; Liu, J.; Chacko, D.; Zhang, K.; Harvey, A. P.; Haribal, V. P.; Zhou, S. J.; Li, F. CexZr1-XO2-Supported CrOx Catalysts for CO2-Assisted Oxidative Dehydrogenation of Propane—Probing the Active Sites and Strategies for Enhanced Stability. *ACS Catal.* **2023**, *13* (1), 213−223.

(53) Xu, B.; Zheng, B.; Hua, W.; Yue, Y.; Gao, Z. Support Effect in Dehydrogenation of Propane in the Presence of CO2 over Supported Gallium Oxide Catalysts. *J. Catal.* **2006**, *239* (2), 470−477.

(54) Michorczyk, P.; Góra-Marek, K.; Ogonowski, J. Dehydrogenation of Propane in the Presence and Absence of CO2 over β-Ga2O3 Supported Chromium Oxide Catalysts. *Catal. Lett.* **2006**, *109* (3−4), 195−198.

(55) Ren, Y.; Wang, J.; Hua, W.; Yue, Y.; Gao, Z. Ga 2O 3/HZSM-48 for Dehydrogenation of Propane: Effect of Acidity and Pore Geometry of Support. *J. Ind. Eng. Chem.* **2012**, *18* (2), 731−736.

(56) Michorczyk, P.; Kuśtrowski, P.; Kolak, A.; Zimowska, M. Ordered Mesoporous Ga2O3 and Ga2O 3-Al2O3 Prepared by Nanocasting as Effective Catalysts for Propane Dehydrogenation in the Presence of CO2. *Catal. Commun.* **2013**, *35*, 95−100.

(57) Zhang, L.; Wang, Z. Y.; Song, J.; Lang, Y.; Chen, J. G.; Luo, Q. X.; He, Z. H.; Wang, K.; Liu, Z. W.; Liu, Z. T. Facile Synthesis of SiO2 Supported GaN as an Active Catalyst for CO2 Enhanced Dehydrogenation of Propane. *J. CO2 Util.* **2020**, *38*, 306−313.

(58) Zheng, B.; Hua, W.; Yue, Y.; Gao, Z. Dehydrogenation of Propane to Propene over Different Polymorphs of Gallium Oxide. *J. Catal.* **2005**, *232* (1), 143−151.

(59) Gashoul Daresibi, F.; Khodadadi, A. A.; Mortazavi, Y. Atomic Layer Deposition of Ga2O3 on γ-Al2O3 Catalysts with Higher Interactions and Improved Activity and Propylene Selectivity in CO2-Assisted Oxidative Dehydrogenation of Propane. *Appl. Catal. A Gen.* **2023**, *655*, 119117.

(60) Dury, F.; Centeno, M. A.; Gaigneaux, E. M.; Ruiz, P. An Attempt to Explain the Role of CO2 and N2O as Gas Dopes in the Feed in the Oxidative Dehydrogenation of Propane. *Catal. Today* **2003**, *81* (2), 95−105.

(61) Chen, M.; Xu, J.; Cao, Y.; He, H. Y.; Fan, K. N.; Zhuang, J. H. Dehydrogenation of Propane over In2O3-Al 2O3Mixed Oxide in the Presence of Carbon Dioxide. *J. Catal.* **2010**, *272* (1), 101−108.

(62) Chen, M.; Xu, J.; Liu, Y. M.; Cao, Y.; He, H. Y.; Zhuang, J. H. Supported Indium Oxide as Novel Efficient Catalysts for Dehydrogenation of Propane with Carbon Dioxide. *Appl. Catal. A Gen.* **2010**, *377* (1−2), 35−41.

(63) Solymosi, F.; Németh, R.; Oszkó, A. The Oxidative Dehydrogenation of Propane with CO2 over Supported Mo2C Catalyst. *Stud. Surf. Sci. Catal.* **2001**, *136*, 339−344.

(64) Dury, F.; Gaigneaux, E. M.; Ruiz, P. The Active Role of CO2 at Low Temperature in Oxidation Processes: The Case of the Oxidative Dehydrogenation of Propane on NiMoO4 Catalysts. *Appl. Catal. A Gen.* **2003**, *242* (1), 187−203.

(65) Kang, J.; Czaja, A. D.; Guliants, V. V. Carbon Dioxide as Feedstock in Selective Oxidation of Propane. *Eur. J. Inorg. Chem.* **2017**, *2017* (40), 4757−4762.

(66) Ascoop, I.; Galvita, V. V.; Alexopoulos, K.; Reyniers, M. F.; Van Der Voort, P.; Bliznuk, V.; Marin, G. B. The Role of CO2 in the Dehydrogenation of Propane over WOx-VOx/SiO2. *J. Catal.* **2016**, *335*, 1−10.

(67) Chung, I.; Jeong, H.; Lee, D.; Oh, J.; Seo, O.; Tayal, A.; Yun, Y. Effect of Mo Content on Oxidative Dehydrogenation of Propane with CO2 over ZnOx Catalysts Supported on Mo−Zr Mixed−Oxides. *Catal. Today* **2024**, *425*, 114340.

(68) Zhang, X.; Li, J.; Liu, W.; Zheng, Y.; An, J.; Xin, W.; Liu, Z.; Xu, L.; Li, X.; Zhu, X. Synergistic Effect of Zinc and Iron in the CO2-Assisted Oxidative Dehydrogenation of Propane. *ACS Catal.* **2023**, *13* (22), 14864−14873.

(69) Jiang, X.; Lis, B. M.; Wu, Y.; Wachs, I. E.; Wu, Z. Effect of the Molecular Structure of Surface Vanadia on Activity and Regenerability of VOx/In2O3 Catalysts for CO2-Assisted Oxidative Dehydrogenation of Propane. *J. Phys. Chem. C* **2023**, *127* (13), 6311−6320.

(70) Zhai, P.; Xie, Z.; Huang, E.; Aireddy, D. R.; Yu, H.; Cullen, D. A.; Liu, P.; Chen, J. G.; Ding, K. CO2-Mediated Oxidative Dehydrogenation of Propane Enabled by Pt-Based Bimetallic Catalysts. *Chem.* **2023**, *9* (11), 3268−3285.

(71) Tóth, A.; Halasi, G.; Bánsági, T.; Solymosi, F. Reactions of Propane with CO2 over Au Catalysts. *J. Catal.* **2016**, *337*, 57−64.

(72) Gomez, E.; Kattel, S.; Yan, B.; Yao, S.; Liu, P.; Chen, J. G. Combining CO2 Reduction with Propane Oxidative Dehydrogenation over Bimetallic Catalysts. *Nat. Commun.* **2018**, *9* (1), 1398.

(73) Guo, J.; Lou, H.; Zhao, H.; Zheng, L.; Zheng, X. Dehydrogenation and Aromatization of Propane over Rhenium-Modified HZSM-5 Catalyst. *J. Mol. Catal. A: Chem.* **2005**, *239* (1−2), 222−227.

(74) Pradhan, S.; Upham, D. C.; Metiu, H.; McFarland, E. W. Partial Oxidation of Propane with CO2 on Ru Doped Catalysts. *Catal. Sci. Technol.* **2016**, *6* (14), 5483−5493.

(75) Gomez, E.; Xie, Z.; Chen, J. G. The Effects of Bimetallic Interactions for CO 2 -assisted Oxidative Dehydrogenation and Dry Reforming of Propane. *AichE J.* **2019**, *65* (8), No. e16670.

(76) Yang, G. Q.; Ren, X.; Kondratenko, V. A.; Zhang, H. B.; Kondratenko, E. V.; Liu, Z. W. Promotional Nature of Sn on Pt/CeO2 for the Oxidative Dehydrogenation of Propane with Carbon Dioxide. *Nano Res* **2023**, *16* (5), 6327−6250.

(77) Wang, H.; Tsilomelekis, G. Catalytic Performance and Stability of Fe-Doped CeO2in Propane Oxidative Dehydrogenation Using Carbon Dioxide as an Oxidant. *Catal. Sci. Technol.* **2020**, *10* (13), 4362−4372.

(78) Xing, F.; Ma, J.; Shimizu, K. I.; Furukawa, S. High-Entropy Intermetallics on Ceria as Efficient Catalysts for the Oxidative Dehydrogenation of Propane Using CO2. *Nat. Commun* **2022**, *13* (1), 5065.

(79) Xing, F.; Nakaya, Y.; Yasumura, S.; Shimizu, K.; Furukawa, S. Ternary Platinum−Cobalt−Indium Nanoalloy on Ceria as a Highly Efficient Catalyst for the Oxidative Dehydrogenation of Propane Using CO2. *Nat. Catal.* **2022**, *5* (1), 55−65.

(80) Carter, J. H.; Hutchings, G. J.; Shah, P. M.; Nowicka, E.; Freakley, S. J.; Morgan, D. J.; Golunski, S. Enhanced Activity and Stability of Gold/Ceria-Titania for the Low-Temperature Water-Gas Shift Reaction. *Front. Chem.* **2019**, *7*, 443.

(81) Pilasombat, R.; Daly, H.; Goguet, A.; Breen, J. P.; Burch, R.; Hardacre, C.; Thompsett, D. Investigation of the Effect of the Preparation Method on the Activity and Stability of Au/CeZrO 4 Catalysts for the Low Temperature Water Gas Shift Reaction. *Catal. Today* **2012**, *180* (1), 131−138.

(82) Cao, P.; Yan, B.; Chu, Y.; Wang, S.; Yu, H.; Li, T.; Xiong, C.; Yin, H. Synthesis of Highly Dispersed Palladium Nanoparticles Supported on Silica for Catalytic Combustion of Methane. *Ind. Eng. Chem. Res.* **2021**, *60* (20), 7545−7557.

(83) Lang, W. Z.; Hu, C. L.; Chu, L. F.; Guo, Y. J. Hydrothermally Prepared Chromia-Alumina (XCr/Al2O3) Catalysts with Hierarchical Structure for Propane Dehydrogenation. *RSC Adv.* **2014**, *4* (70), 37107−37113.

(84) Weckhuysen, B. M.; Schoonheydt, R. A. Alkane Dehydrogenation over Supported Chromium Oxide Catalysts. *Catal. Today* **1999**, *51* (2), 223−232.